OpenAIR @RGU | ROBERT GORDON UNIVERSITY ABERDEEN

This publication is made freely available under GREEN open access.

AUTHOR(S): WANG, S., FERNANDEZ, C., SHANG, L., LI, Z. and LI, J.

TITLE: Online state of charge estimation for the aerial lithium-ion battery packs based on the improved extended Kalman filter method.

YEAR: 2017

Publisher citation: WANG, S., FERNANDEZ, C., SHANG, L., LI, Z. and LI, J. 2017. Online state of charge estimation for the aerial lithium-ion battery packs based on the improved extended Kalman filter method. Journal of energy storage [online], 9, pages 69-83. Available from: https://doi.org/10.1016/j.est.2016.09.008

OpenAIR citation: WANG, S., FERNANDEZ, C., SHANG, L., LI, Z. and LI, J. 2017. Online state of charge estimation for the aerial lithium-ion battery packs based on the improved extended Kalman filter method. Journal of energy storage, 9, pages 69-83. Held on OpenAIR [online]. Available from: https://openair.rgu.ac.uk

Publisher copyright statement:

This is the AUTHOR ACCEPTED version of an article originally published by ELSEVIER in Journal of energy storage (ISSN 2352-152X; eISSN _____).

OpenAIR takedown statement:

Section 6 of the "Repository policy for OpenAIR @ RGU" (available from http://www.rgu.ac.uk/staff-and-current-students/library/library-policies/repository-policies) provides guidance on the criteria under which RGU will consider withdrawing material from OpenAIR. If you believe that this item is subject to any of these criteria, or for any other reason should not be held on OpenAIR, then please contact openair-help@rgu.ac.uk with the details of the item and the nature of your complaint.

This publication is distributed under a CC BY-NC-ND 4.0 license.

https://creativecommons.org/licenses/by-nc-nd/4.0

OpenAIR at RGU

Digitally signed by OpenAIR at RGU
DN: cn=OpenAIR at RGU, o=Robert Gordon University, ou=Library, email=publications@rgu.ac.uk, c=GB
Date: 2018.02.22 10:51:24 Z

Online state of charge estimation for the aerial lithium-ion battery packs based on the improved extended Kalman filter method

Shunli Wang[a], Carlos Fernandez[b], Liping Shang[a], Zhanfeng Li[c], Jianchao Li[d]

[a]*School of Information Engineering & Robot Technology Used for Special Environment Key Laboratory of Sichuan Province, Southwest University of Science and Technology, Mianyang 621010, China;*
[b]*School of Pharmacy and Life Sciences, Robert Gordon University, Aberdeen AB10-7GJ, UK;*
[c]*School of Manufacturing Science and Engineering, Southwest University of Science and Technology, Mianyang 621010, China;*
[d]*MianYang Product Quality Supervision & Inspection Institute, Mianyang 621000, China*

Abstract: An effective method to estimate the integrated state of charge (SOC) value for the lithium-ion battery (LIB) pack is proposed, because of its capacity state estimation needs in the high-power energy supply applications, which is calculated by using the improved extended Kalman filter (EKF) method together with the one order equivalent circuit model (ECM) to evaluate its remaining available power state. It is realized by the comprehensive estimation together with the discharging and charging maintenance (DCM) process, implying an accurate remaining power estimation with low computational calculation demand. The battery maintenance and test system (BMTS) equipment for the aerial LIB pack is developed, which is based on the proposed SOC estimation method. Experimental results show that, it can estimate SOC value of the LIB pack effectively. The BMTS equipment has the advantages of high detection accuracy and stability and can guarantee its power-supply reliability. The SOC estimation method is realized on it, the results of which are compared with the conventional SOC estimation method. The estimation has been done with an accuracy rate of 95% and has an absolute root mean square error (RMSE) of 1.33% and an absolute maximum error of 4.95%. This novel method can provide reliable technical support for the LIB power supply application, which plays a core role in promoting its power supply applications.

Keywords: *aerial lithium-ion battery; improved extended Kalman filter; state of charge; optimal prediction; comprehensive estimation*

Corresponding author: Shunli Wang. Tel/fax: +86-15884655563. E-mail address: wangshunli@swust.edu.cn.

1. Introduction

The accurate SOC estimation is a core factor of a variety of applications for the LIB-based energy storage and supply systems. Because of their high energy, high power, long cycle life and low purchase price when compared with other battery types such as lead acid and nickel cadmium batteries, the LIB has become popular in many energy-powered applications. For the high reliability requirement characteristics of aviation application, the LIB packs are used as alternate emergency equipment in the aerial control system. It is used to solve the instantaneous energy shortage problems and provide the energy supply protection for other emergency situations. Because of its high energy density advantage, the LIB packs are increasingly used in the aerial applications, which are becoming to substitute the nickel-cadmium batteries to be the main power supply batteries.

With respect to the cell continuous mutation in the high power supply aerial LIB packs, the SOC value should be estimated real-time accurately in the approximated BMS equipment and becomes an increasingly challenging problem that requires rigorous calculation limits. Especially in the aircraft environment, the actual SOC estimation of the LIB pack is rather a crucial factor to be predicted accurately. As the ECM is commonly used to assess the performance of the LIB electric-power operating state, the dynamic and closed-loop model named as EKF combining with ECM is extensively used in the SOC estimation process of the power LIB packs, reducing the computational requirements in the traditional SOC estimation method. The on-line adaptive battery impedance parameter and state estimation is conducted by Fleischer et al. (2014) considering physical principles in reduced order ECM battery models. The relationship between SOC and OCV is usually used for the SOC value correction in the accessional BMS real-time control application of the power LIB packs. The improved SOC estimation method is proposed in this paper, which is based on the real-time online ECM electrolysis parameters. The stage optimization for cascade and optimized EKF approach is used for the accurate SOC estimation, which is suitable

for the BMS control in the aerial LIB pack power supply applications due to its simplicity computational process. The symbols used in the paper can be described in Tab.1.

Tab.1 List of symbols

Symbol	Description	Symbol	Description
LIB	Lithium-Ion Battery	EKF	Extended Kalman Filter
KF	Kalman Filter	BMS	Battery Management System
SOC	State of Charge	SEI	Solid Electrolyte Interface
DCM	Discharging and Charging Maintenance	PNGV	Partnership for New Generation of Vehicles
OCV	Open Circuit Voltage	HPPC	Hybrid Pulse Power Characterization Test
ECM	Equivalent Circuit Model	Ah	Ampere hour
EVs	Electric Vehicles	MMSE	Minimum Mean Square Error
CC	Constant Current	CV	Constant Voltage
BMTS	Battery Maintenance and Testing System	ANN	Artificial Neural Network
NN	Neural Network	SVM	Support Vector Machine
RC	Resistor-Capacitor	NASA	National Aeronautics and Space Administration
EIS	Electro-chemical Impedance Spectroscopy	UKF	Unscented Kalman Filter

During the lifetime of the aerial LIB, the capacity and SOC values of the individual battery cell will change along with the electrochemical degradation process, due to the decomposition of the electrolytes and the SEI growth of the anode surface. These variables are difficult to measure directly in the aircraft control system, but they should be aware of the precise scope to know its energy state. The aircraft control system undergoes the over-charging, over-discharging, over-temperature and limited energy acceleration risks with no SOC correction and control that can be done by the assorted BMS of the aerial LIB pack. Because of the positive correlation relationship that is existed in the energy consumption and weight in the aircraft, the high energy density is an important basis for the battery selection of the performance indicators. However, because of the aircraft 787 incidents spontaneous events caused by the combustion event of the LIB pack, the high stability and reliability advantages of power LIB packs are worried and questioned, restricting power LIB pack application seriously.

Due to reliable SOC prediction necessity and urgent needs, a lot of research work has been done on it in last few years. Kim J et al. (2015) studied the DCM to increase the capacity and SOC prediction accuracy, in which the voltage-temperature pattern is recognized at various temperatures based on the Hamming network-dual EKF application. These smart approaches are particularly dependent on the training samples and the estimation accuracy decreases seriously when the LIB cell performance changes. Andre D et al. (2015) tries the standard KF interaction and UKF combined SVM for the SOC estimation of LIBs by the detailed deduction algorithm. There are many other researchers in this field to conduct in-depth research as well. The SOC estimation of LIB using square root spherical UKF is conducted by Aung el al. (2015) in the nano-satellite. The temperature dependent SOC estimation of LIB using dual spherical UKF is studied by Aung et al. (2015). The OCV characterization technique and hysteresis assessment is studied by Barai et al. (2015) of LIB cells. The electrochemical model-based SOC and capacity estimation algorithm is studied by Bartlett et al. (2016) for the composite electrode LIB. The experimental study is conducted by Bazinski et al. (2015) on the influence of temperature and SOC for the thermo-physical properties of the LIB cell. The particle-filtering-based estimation of maximum available power state is conducted by Burgos-Mellado et al. (2016) in LIBs. The SOC estimation for the LIB is conducted by Chen et al. (2016) with a robust adaptive sliding-mode observer using RBF NN algorithm in EVs. The electrochemical model-based SOC estimation is conducted by Corno et al. (2015) for Li-ion cells. The OCV-based SOC estimation is conducted by Dang et al. (2016) for the LIB using dual NN fusion battery model. The online SOC estimation and OCV hysteresis modeling of LIB is conducted by Dong et al. (2016) using invariant embedding method. The discrete wavelet transform-based de-noising technique is studied by Lee et al. (2015) for the advanced SOC estimator of the LIB in EVs. However, the SOC estimation of high power LIB packs still lack of effect systematic methods. In order to adapt to different working environments, deterministic models have been used, especially in high safety applications like EV or HEV to avoid the SOC estimation failure. At the same time, it is necessary to track the error in the BMS, which should be also used attached the LIB pack for the real-time correction and self-learning dynamic traction by using the KF-based SOC estimation method.

A novel SOC estimation method is proposed for the aerial LIB pack available energy assessment based on the DCM algorithm, providing a comprehensive remaining capacity state estimation of the LIB pack. Even if the aging

mechanism or source can be obtained from the SOC estimation algorithm, there is no direct understanding that may be a collection of information on the deterioration of specific aging factors. Therefore, the main factors of LIB working status can be identified and determined. A brief description of the mathematical method used in this approach is given after the theoretical guidance and presentation of the SOC estimation. Then, the design and implementation of BMTS equipment is done to estimate the real-time SOC of the LIB pack.

2. The real-time battery model

In this section, a brief description of the mathematical method applied to this study is given. The LIB is classified as lithium ion cobalt oxide, lithium ion manganese oxide, lithium iron phosphate and other types of batteries according to the type of anode material. Lithium cobalt oxide has been used in the aircraft and other areas of the pilot application, due to its high energy density, good safety and reliability, etc. The proposed SOC estimation method based on EKF and DCM plays an important role in promoting the application of the LIB pack.

2.1. The DCM mechanism of the aerial LIB cell

Due to the perspective of the material, the aerial LIB cell is composed of a positive electrode, a separation, a negative electrode and the organic electrolyte, the different parts of which are shown as follows. The most positive electrode active material is cobalt oxide. The polymer separator is a special kind of molding, the micro-porous structure of which allows the free passage of the lithium ion, while blocking the electrons. The active material of the graphite anode is carbon graphite or other similar structural materials, which can be used as conductive electrolytic lithium-ion collectors. Excessive charging and discharging of LIB will lead to irreversible damage to the battery which reduces its performance and lifetime. The organic solvent of the electrolyte is carbonate. The shape and size of the battery shell are steel and square. The internal reaction of LIB in its DCM process is shown in Fig. 1.

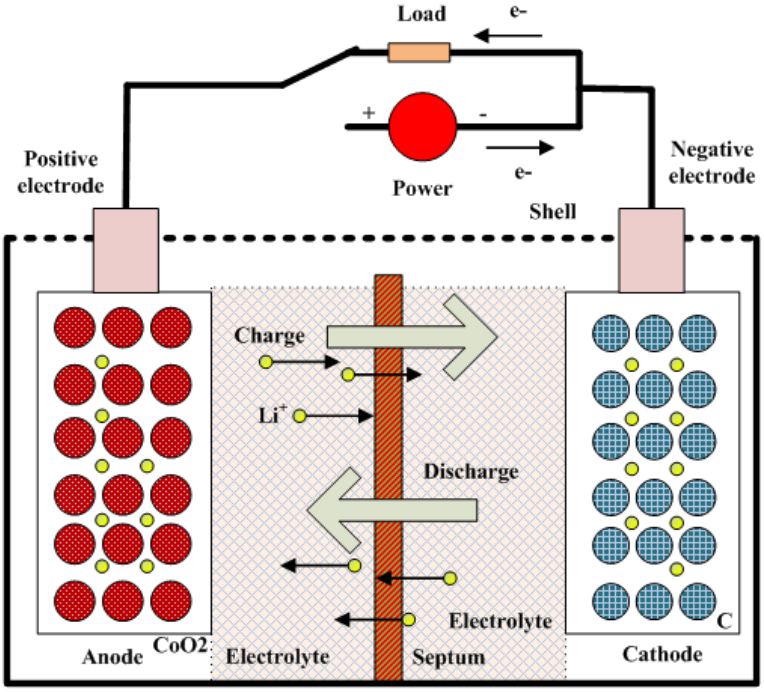

Fig. 1. Discharging and charging mechanism of the LIB cell

The LIB attracts more and more attention as an green energy source with the development of lithium-ion components and materials, which is mainly due to the high energy, high power density and long cycling life advantages. The intelligent monitoring system is used to estimate the SOC value of the LIB pack accurately. When the LIB pack is in the working process of the emergency power supply, the two electrodes are connected to an open module, which can be described as shown in Fig. 2.

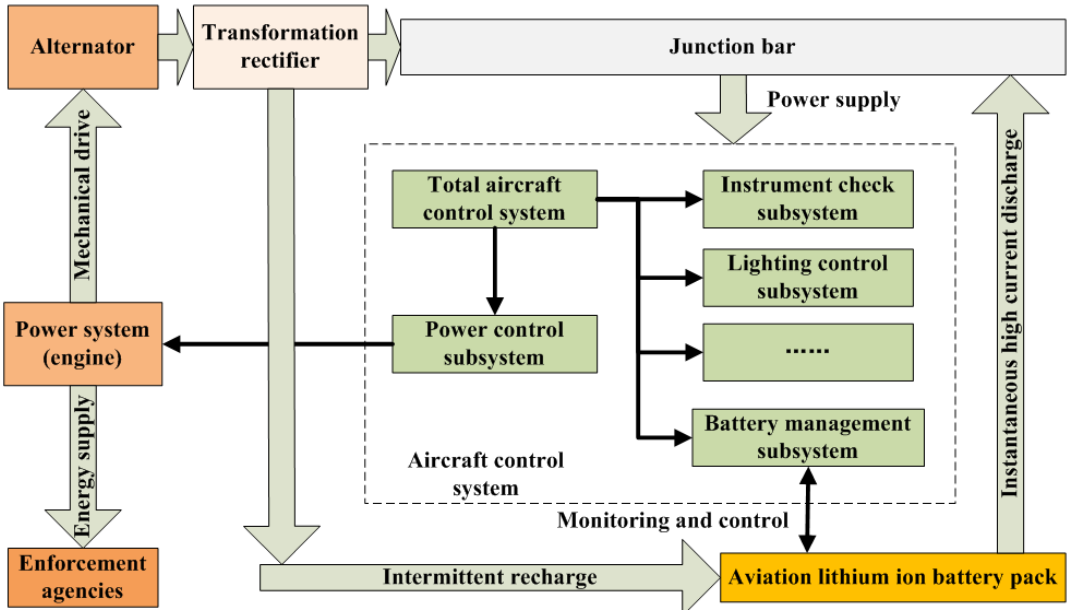

Fig. 2. Aerial LIB pack energy supply principle

Then, the data download module and critical load equipment may constitute a closed circuit. Because of the potential difference effect, the electrons travel from the cathode to the anode outside the LIB cell. Meanwhile, the lithium ions travel from the negative electrode to the positive electrode, through the electrolyte and a separator in the internal LIB cell until the lithium-rich plasma state appears. The OCV characterization is studied by pattipati et al. (2014) for LIBs. Lithium ions travel from the cathode to the anode, until the lithium ion thin the state appears, in which the electrolyte solution is immersed in to these two identical current flows between the electrodes. The overall reaction of the cathode against the negative electrode reaction is displayed as follows.

$$\begin{cases} Anode: LiCoO_2 \underset{\text{discharge}}{\overset{\text{charge}}{\rightleftarrows}} Li_{1-x}CoO_2 + xLi + xe^- \\ Cathode: xLi + xe^- + 6C \underset{\text{discharge}}{\overset{\text{charge}}{\rightleftarrows}} Li_xC_6 \\ Total: LiCoO_2 + 6C \underset{\text{discharge}}{\overset{\text{charge}}{\rightleftarrows}} Li_{1-x}CoO_2 + Li_xC_6 \end{cases} \quad (1)$$

2.2. The ECM for the LIB characterization

In order to maintain the safety and performance of the LIB, a reliable and accurate SOC estimation method is necessary for modern BMS. The SOC is a crucial factor that shows the remaining battery capacity and system to help predict the remaining driving range of the spectrum. More importantly, the precise SOC estimation can prevent the LIB pack from the over-charge and over-discharge risks that will damage the battery and brings in danger for the aerial power supply system, making it to be an important role in the aircraft control systems. Mounts of SOC estimation methods for the on-chip management systems have been proposed, in which the Coulomb counting method is the most popular because of its simplicity and low computational cost. The electrochemical machining method uses the resistors, capacitors and other electrical components for the LIB equivalent modeling, it is very simple to achieve and can capture the dynamic response to the LIB accurately, making it applicable to the LIB control and simulation purposes.

The Coulomb counting algorithm is an open loop estimation, the accuracy of which depends on the accuracy of the sensor and suffered from the initial error and measurement error accumulation, because it depends on the current flowing out of the LIB cell unit. The SOC estimation method includes current integration, OCV corresponding, and filtering methods based on black box method and model. Each method has its own advantages

and disadvantages. The current integration method is simple and low computational effort to achieve, but the estimation accuracy is reduced, because of the accumulated current error due to the sensor noise.

Black box model-based approaches typically use a black box model training data, such as neural networks and support vector regression, the estimated value of its systems. The estimation may be quite accurate with particularly high computational effort, if there is enough training data offline. Model-based filtering method is usually used in the state space model and is considered to be the most promising method to estimate the SOC of the LIB, because of the high estimation accuracy and error correction capability online advantages. A simplified PNGV battery model is proposed for the high power LIB cell, aiming to characterize it and obtain the state-space equations for the SOC estimation. The accurate SOC estimation model can be constructed according to the draw HPPC curve, calculated OCV-SOC, ECM and battery parameters.

The SOC estimation method is based on the state-space equation, such as a sliding mode observer, security, EKF and UKF, etc., have been used in SOC estimation. ECM has been widely used, unlike the estimated long-term aging of on-board chip. A large number of studies have been done on the LIBS modeling the ECM. The model-based condition monitoring is conducted by Kim et al. (2015) for the LIBs. The LIB pack is usually composed of many cells in order to meet high capacity requirements and provide the required voltage for the high power energy supply applications, which are connected in series and parallel. It is based on the assumptions that the behavior of all the cells in the package. Therefore, the LIB pack can easily be modeled as a unit cell having higher voltage and larger capacity. In its simplest form, the LIB cell has been proposed in a very complex form, the electrical and electrochemical behaviors of which can be obtained and shown in Fig.3. The ECM consist of the resistance and capacitance values can be achieved by using different techniques, such as EIS and pulse power testing. These techniques can be well understood and described by the general relationship between the different real-world working conditions of the circuit parameters.

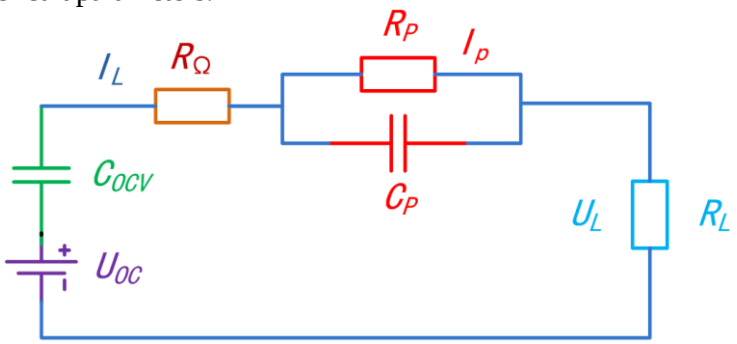

Fig. 3. The ECM for the LIB characterization

The above figure shows the polarization model of a LIB cell and there are some parameters should be known in the figure. The resistor R_Ω represents the instantaneous voltage drop during the battery ECM process. The RC network composed by the parameter R_P and C_P is used to model the relaxation effects of LIB in the DCM process. The RC network models the short term transient response of LIB and the long term transient response. In the ECM, the parameter U_{OC} represents the OCV, the parameter U_L represents the terminal voltage of LIB and the parameter I_L represents the LIB current. In general, it provides good modeling accuracy and has simple structure, less computation and fast processing speed advantages. As the production variability and uneven working environment cannot be avoided, the thermal and energy imbalance exists in the DCM process. The SOC identification is essential when the OCV path dependence lags a distinctive feature and its exact estimation are correct. Experimental results show that the OCV and capacity value of the LIB is directly related to DCM working conditions. A dynamic hysteresis model is used to obtain better accuracy for the SOC estimation, which can be realized on-chip in the associated BMS equipment, rather than using the Ah integral method. The results show the importance of the OCV characterization in the experimental test program.

The difference among the connected cells should be a big problem, which makes the cell ECM model do not fit the LIB pack. In addition, the battery pack and the ability to store energy chip and transmission power, so the

system is highly dependent on the performance of every single cells. A real-time joint estimator is constructed by Gao et al. (2015) for model parameters and SOC of LIBs in EVs. The state equation can be obtained by the analysis of Fig.3. A systematic review is conducted by Nejad et al. (2016) for the LIB state real-time estimation of lumped-parameter ECMs. It has just one RC circuit to simply the computational complexity, compared with the multiple RC circuit ECM used by Wang L et al. (2015) as shown in Fig.1 and the two order RC circuit used by Tong SJ et al. (2015).

$$U_L = U_{OC} - C_b\left(\int I_L dt\right) - R_\Omega I_L - R_p I_p \tag{2}$$

In the HPPC experiment, the parameters of *a*, *b*, *c* and *d* are selected as four different sample time moments and the Eq.3 can be obtained accordingly.

$$\begin{bmatrix} V_{OC} \\ C_b \\ R_O \\ R_P \end{bmatrix} = \begin{bmatrix} 1 & \int_0^a I_{L,a} dt & I_{L,a} & I_{P,a} \\ 1 & \int_0^b I_{L,b} dt & I_{L,b} & I_{P,b} \\ 1 & \int_0^c I_{L,c} dt & I_{L,c} & I_{P,c} \\ 1 & \int_0^d I_{L,d} dt & I_{L,d} & I_{P,d} \end{bmatrix} \begin{bmatrix} V_{L,a} \\ V_{L,b} \\ V_{L,c} \\ V_{L,d} \end{bmatrix} \tag{3}$$

The parameter of U_{OC} represents the open-circuit voltage of lithium batteries. The parameter of C_b represents the line equivalent capacitance. The parameter of R_O represents the line equivalent resistance. The parameter of R_P represents the internal equivalent resistance of the battery. The parameter of I_L is on behalf of the line current. The parameter of I_P represents the current flowing through the resistance. The parameter V_L indicates the external load terminal voltage of lithium batteries. The subscript of *a*, *b*, *c* and *d* denote four different sample times, which are used as time parameters to characterize different state values.

The open circuit voltage U_{OC} parameter of LIB has a nonlinear relationship with SOC. In order to obtain a non-linear function, the OCV testing was performed using and aerial LIB packs with 45Ah as the experimental samples. Hysteresis effect in this study is neglected by assuming that there is an additional voltage source in parallel with the digital parameters U_{OC} increased complexity. The CC-CV charging method is used for the LIB packs. Then, it is set to be rest for an hour to make it in the steady state and the parameters are measured by the fully charged state at the end of the rest. In the different level SOC measurement successor is designed more than an hour, rest for one hour when the experimental LIB reaches a steady state, so that the SOC-OCV relationship can be obtained from the series experiments. The OCV value of the LIB is directly related to the DCM working conditions and the polynomial fitting curves can be used to describe the relationship between the OCV and SOC, in which the obtained sufficient error norm is 0.01 by using a seven-order equation. The SOC-OCV relations will be used in the next section, the estimated terminal voltage lithium-ion battery. The state-space equation of the LIB can be obtained and expressed in discrete time as shown in Eq.4.

$$SOC(k+1) = SOC(k) - \frac{\eta I_L \Delta t}{Q_d} \tag{4}$$

Wherein, the parameter Q_d is the discharging capacity of the LIB and the parameter I_L is the discharging current of the LIB. Meanwhile, the parameter $\triangle t$ is the sampling time and the parameter η is the Coulomb efficiency. The circuit dynamics of the RC network can be rewritten as shown in Eq.5 by using the Kirchhoff circuit law.

$$\frac{dU_P}{dt} = -\frac{U_P}{R_P C_P} + \frac{I_L}{C_P} \tag{5}$$

The LIB state-space equation can be obtained by taking $[SOC\ U_P]^T$ as the state variables, which can be described in Eq.6.

$$\begin{bmatrix} SOC_{k+1} \\ U_{Pk+1} \end{bmatrix} = F\left(SOC, U_P\right) = \begin{bmatrix} 1 & 0 \\ 0 & e^{-\frac{\Delta t}{R_P C_P}} \end{bmatrix} \times \begin{bmatrix} SOC_k \\ U_{Pk} \end{bmatrix} + \begin{bmatrix} -\frac{\Delta t}{Q_d} \\ R_P\left(1 - e^{-\frac{\Delta t}{R_P C_P}}\right) \end{bmatrix} \left[I_L\right] \tag{6}$$

The LIB terminal voltage U_L is set as the system output and the LIB current I_L is set as the system input, then, the measurement function H for the output signal U_L can be obtained as shown in Eq.7.

$$U_L = H\left(f\left(SOC\right), U_P\right) = \begin{bmatrix} 1 & -1 \end{bmatrix} \begin{bmatrix} f\left(SOC\right) \\ U_P \end{bmatrix} - I_L R_\Omega \tag{7}$$

In order to estimate the parameters of *SOC* and U_P, the LIB parameters of R_Ω, R_P and C_P are required, which will be experimentally identified and discussed afterwards. Transfer function method is introduced and applied to the library parameters required for recognition. Through the above analysis, the preparation can be obtained at the free end of the voltage in the frequency domain as shown in Eq.8.

$$U_L\left(s\right) = U_{OC}\left(s\right) - I_L\left(s\right) R_\Omega - \frac{R_P I_L\left(s\right)}{1 + R_P C_P\left(s\right)} \tag{8}$$

The output voltage U_L and open circuit voltage U_{OC} difference parameter as the output current I_L and set the parameters as input parameters, the transfer function G(s) can be obtained as shown in Eq.9. The OCV value is the free thermodynamic equilibrium potential with no current and connected loads. The OCV is an important feature as a function of the ECM for the SOC estimation. As an ideal, but a variable voltage source, electrolysis process in the electrolytic machining over-potential increased residual resistance and capacitive elements. Instead, a lithium-ion battery SOC based on the open circuit voltage of the battery is known, this is the key to the system. One to one relationship between the open-circuit voltage and the SOC, and is generally considered to use, however, due to the lag exists, LIB battery open circuit voltage of the DCM process changes. Any lag thus implying potential LIB battery open circuit voltage, insufficient knowledge of history do not understand the characterization of free Cell DCM to determine the SOC value.

$$G\left(s\right) = \frac{U_L\left(s\right) - U_{OC}\left(s\right)}{I_L\left(s\right)} = -\frac{a_2 s^2 + a_1 s + a_0}{s^2 + b_1 s + b_0} = -\frac{R_\Omega s^2 + \left(\frac{R_\Omega}{R_P C_P} + \frac{1}{C_P}\right) s + \frac{R_\Omega + R_P}{R_P C_P}}{s^2 + \frac{1}{R_P C_P} s + \frac{1}{R_P C_P}} \tag{9}$$

Power supply applications free library package from a single cell is composed of a combination of series and parallel. Batteries in parallel to meet the high capacity requirements and provide the required system voltage in the series. The influence of memory effect on the SOC estimation is conducted by Shi et al. (2016) for large format LIBs based on LiFePO4 cathode. In a pack, the battery capacity and internal resistance of the battery parameters, from cell to cell due to manufacturing variation, aging, and different operating conditions, such as temperature gradients within the package. The SOC modeling is conducted by Kuo et al. (2016) for the LIBs using dual exponential functions. Changes in the battery voltage, capacity, internal resistance and the sheet of the available energy adversely affect the battery system, reducing battery performance and life. Therefore, different from the BMS balance control method for treating cell changes, thereby improving battery performance. The model based condition monitoring is conducted by Singh et al. (2014) in LIBs. The detection and the date of the forecast date in fig.4. are shown in the figure we can see, as a predictor of a good agreement, have the detection with SOC. In the present study, the combination of PNGV model is used, the simulation model of which is shown in Fig. 4.

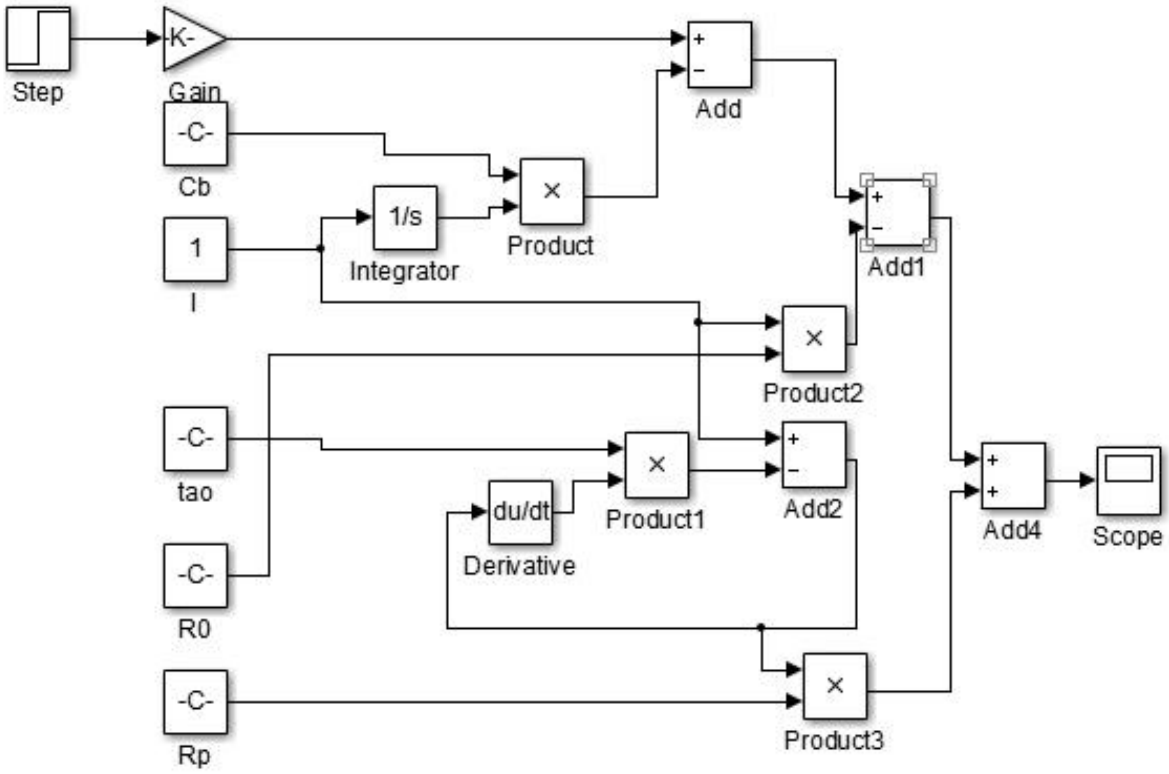

Fig. 4. The simulation model for the ECM of LIB

2.3. The SOC estimation model construction

A recursive solution can be provided by using the KF algorithm to estimate the state by a linear optimal filter system variables. This method is widely used in SOC estimation process, can well be combined with other observers and estimation algorithms include Neural Network. However, it is the experience of limitations such as stability and precision filter, improved EKF introduced aimed at reducing dependency on computing Jacobian matrix, wherein the weighted point estimates free sample mean and covariance. If the estimated parameter vector changes slowly change over time or a change of time estimated to the estimation it can be named. Meanwhile, if the estimated parameter vector change over time, the estimated dynamic estimation can be named. From the battery equivalent circuit model may know, it is estimated that the process of on-chip system is the dynamic estimation. In practical engineering problems, there are many signals are noise pollution. Assume parameter $X(t)$ is a useful signal, parameter random noise parameter V(t), and then the detection signal $Z(t)=X(t)+V(t)$, which is superimposed on the useful signal and noise signal. KF algorithm for linear discrete stochastic system can be described as follows. Discrete stochastic linear systems can be assumed to be shown in Eq.10.

$$\begin{cases} X(k+1) = \Phi(k+1,k)X(k) + G(k+1,k)U(k) + \Gamma(k+1,k)W(k) \\ Y(k) = H(k)X(k) + V(k) \end{cases} \tag{10}$$

Wherein,

$X(k)$——n dynamical state vector.

$U(k)$——r dynamical control vector.

$W(k)$——p dynamical random interference noise vector.

$Y(k)$——m dynamical observation vector.

$V(k)$——m dynamical random observation noise vector.

EKF algorithm is widely used in SOC estimation, linear approximation of nonlinear function but it increases the complexity of implementation. An adaptive remaining energy prediction approach is proposed by Wang et al.

(2016) for LIBs in EVs. A SOC estimation method is proposed by Wang et al. (2015) for LIBs based on multi-model switching strategy. The dynamic battery cell model and SOC estimation is done by Wijewardana et al. (2016). The model parameter estimation approach is proposed by Wu et al. (2015) based on incremental analysis for LIBs without using OCV. The dimension of the coefficient matrix is shown in Eq.11.

$$\begin{cases} \Phi(k+1,k) \Rightarrow n \times n; G(k+1,k) \Rightarrow n \times r; \\ \Gamma(k+1,k) \Rightarrow n \times p; H(k) \Rightarrow m \times n; \end{cases} \tag{11}$$

The parameters of $W(k)$ and $V(k)$ are zero mean white noise or Gaussian white noise series and they are independent with each other. The enhanced closed loop SOC estimator is constructed by Perez et al. (2015) for the LIBs based on the EKF algorithm. A novel on-board SOC estimation method is proposed by Sepasi et al. (2014) for aged LIBs based on the model adaptive EKF algorithm. Detected inside, they are a constant value, which is characterized as shown in Eq.12.

$$\begin{cases} E\{W(k)\} = 0, Cov\{W(k), W(j)\} = Q_k \delta_{kj} \\ E\{V(k)\} = 0, Cov\{V(k), V(j)\} = R_k \delta_{kj} \\ Cov\{W(k), V(j)\} = 0 \\ if\ (k = j)\{\delta_{kj} = 1\}; else\{\delta_{kj} = 0\}. \end{cases} \tag{12}$$

The parameter Q_k is $p \times p$ dimensional nonnegative definite matrix, which is the variance matrix of the parameter $W(k)$. The parameter R_k is $m \times m$ dimensional positive definite matrix, which is the variance of the parameter $V(k)$. The improved EKF approach is proposed by Sepasi et al. (2014) for the SOC estimation of battery pack. The on-line estimation of SOC of LIBs in EV is conducted by Shao et al. (2014) using the re-sampling particle filter. The statistical properties of the initial value $X(0)$ for the parameter of state vector $X(k)$ are shown in Eq.13.

$$\begin{cases} E\{X(0)\} = \mu_0 \\ Var\{X(0)\} = E\left\{\left[X(0) - \mu_0\right]\left[X(0) - \mu_0\right]^T\right\} = P_0 \end{cases} \tag{13}$$

The LIB security guaranteeing method is studied by Wang et al. (2015) based on the SOC estimation. The elimination is studied by Wang et al. (2015) for the SOC errors of distributed battery energy storage devices in islanded droop-controlled micro-grids. The modeling analysis of dual KF is studied by Wang et al. (2014) in SOC estimates of LIB. The initial value $X(0)$ is unrelated with the parameter $W(k)$ and $V(k)$, which is shown in Eq.14.

$$E\{W(k), X(0)\} = 0, E\{V(t), X(0)\} = 0 \tag{14}$$

The SOC estimation for LIB based on the strong tracking sigma point KF algorithm is studied by Li et al. (2015). A mixed SOC estimation algorithm is proposed by Lim et al. (2016) with high accuracy in various driving patterns of EVs. The probability based remaining capacity estimation is conducted by Wang et al. (2016) using data-driven and NN model. For the system described by the state equation and measurement equation, the observation sequence of $Z(0)$, $Z(1)$, …, $Z(k)$ can be given and it is necessary to find the linear optimal estimation $X(j|k)$ for the parameter $X(j)$ to make the error variance to be minimum which is shown in Eq.15.

$$E\left\{\left[X(j) - \hat{X}(j \mid k)\right]^T \left[X(j) - \hat{X}(j \mid k)\right]\right\} = \min \tag{15}$$

It is also means that all the state variable estimation error variance is required to be minimum. The SOC imbalance estimation is conducted by Lin et al. (2015) for battery strings under reduced voltage sensing. A geometrical approach is proposed by Lu et al. (2014) for the LIB capacity estimation. The SOC estimation for LIB is studied by Meng et al. (2016) based on adaptive UKF and SVM. Meanwhile, the estimation is required to be the linear function of the observation vector $Z(0)$, $Z(1)$, …, $Z(k)$ and the estimation is unbiased as shown in Eq.16.

$$E\left\{\hat{X}(j \mid k)\right\} = E\{X(j)\} \tag{16}$$

The fading KF-based real-time SOC estimation is conducted by Lim et al. (2016) in the LIB-powered EVs. A novel multi-model probability battery SOC estimation approach is proposed by Lin et al. (2016) for EVs using the H-infinity algorithm. A systematic SOC estimation framework is constructed by Sun et al. (2016) for the multi-cell battery pack in EVs using bias correction technique. In the derivation of the Kalman prediction, it is necessary to consider not affect the control signal, so that U(k) = 0, then the discrete linear system can be described as Eq.17.

$$\begin{cases} X(k+1) = \Phi(k+1,k)X(k) + \Gamma(k+1,k)W(k) \\ Y(k) = H(k)X(k) + V(k) \end{cases} \tag{17}$$

Wherein, the parameters of W(k) and V(k) are zero mean white noise series and independent with each other. In the detection interval process, they are constant value and the statistical properties of the initial value of the state vector $X(0)$ is set in advance. The observation sequence of $Y(0)$, $Y(1)$, …, $Y(k)$ can be given, aiming to find the linear optimal estimation $X(k+1|k)$ for the parameter $X(k+1)$ to make the error variance to be minimum. Then, the orthogonal principle and mathematical induction method are used to do the derivation of the Kalman predication estimation functions. When the observation values of $Y(0)$, $Y(1)$, …, $Y(k\text{-}1)$, it is reasonable to assume that the optimal linear prediction estimation for the state vector $X(k)$ is found. When the new observation value $Z(k)$ for k time point is not obtained, how the state vector $X(k+1)$ estimation for $k+1$ time point can be done according to the existing observation values is analyzed. As can be found from the system state function, because the parameter $W(k)$ is a unpredictable white noise sequence, the equation below can only be chosen to do the prediction estimation for the system state vector $X(k+1)$ that is shown in Eq.18.

$$\hat{X}(k+1|k-1) = \Phi(k+1,k)\hat{X}(k|k-1) \tag{18}$$

The improved adaptive SOC estimation is conducted by Fang et al. (2014) for batteries using a multi-model approach. When the parameter $X(k|k+1)$ is the optimal linear estimation of the state vector X(k), then the estimation $X(k+1|k\text{-}1)$ should be the optimal linear prediction of $X(k+1)$. The optimal linear prediction for the observation vector $Z(k)$ at the k time point can be obtained by using the function $Y(k)=H(k)X(k)+V(k)$ as shown in Eq.19.

$$\hat{X}(k|k-1) = H(k)X(k-1) \tag{19}$$

When $X(k|k\text{-}1)$ is the optimal linear estimation of $X(k)$, the estimation $X(k+1|k\text{-}1)$ is also the optimal linear prediction of the parameter $X(k+1)$ which can be proved by the orthogonal theorem. A novel SOC estimation method is proposed by Xia et al. (2014) for LIBs using a nonlinear observer. The SOC is estimated by Xie et al. (2016) for LIBs using an H-infinity observer with consideration of the hysteresis characteristic. By substituting the Eq.18 from Eq19, the estimation equation can be obtained as shown in Eq.20.

$$\hat{X}(k+1|k-1) = \Phi(k+1,k)H(k)X(k-1) \tag{20}$$

A modified model based SOC estimation is conducted by Tian et al. (2014) for the power LIBs using the UKF algorithm. The on-line optimization of battery OCV is done by Tong et al. (2015) for improved SOC and SOH estimation. The SOC estimation and uncertainty is conducted by Truchot et al. (2014) for the LIB strings. The battery SOC estimation is conducted by Unterrieder et al. (2015) using approximate least squares. The battery available power prediction of HEV is conducted by Wang et al. (2014) based on improved Dynamic Matrix Control algorithms. By extracting the common factor $\Phi(k+1,k)$, the estimation error X_e function can be converted into Eq.21.

$$\begin{cases} X_e(k+1|k-1) = \Phi(k+1,k)X_e(k|k-1) + \Gamma(k+1,k)W(k) \\ X_e(k|k-1) = X(k) - \hat{X}(k|k-1) \end{cases} \tag{21}$$

As X(k|k-1) is the optimal linear prediction estimation of X(k), according to the orthogonal theorem, the estimation error as shown in Eq.17 should be orthogonal with the vector sequence $Y(0)$, $Y(1)$, …, $Y(k\text{-}1)$. As a result, its linear conversion by multiplying $\Phi(k+1,k)$ also should be orthogonal with the vector sequence. The parameter $W(k)$ is zero mean white noise sequence and independent with the vector sequence $Y(0)$, $Y(1)$, …, $Y(k\text{-}1)$. As a result, the estimation $X(k+1|k\text{-}1)$ is also the optimal linear prediction of the parameter $X(k+1)$. Then, it is necessary

to study how to amend the prediction estimation $X(k+1|k-1)$ for $X(k+1)$ when the new observation value $Y(k)$ is obtained. If the new observation value $Y(k)$ equals to the prediction estimation $Y(k|k-1)=H(k)X(k|k-1)$ for $Y(k)$, the new prediction value $Y(k)$ does not supply any useful new message for the amending process. It can be proved if the orthogonal relationship between the estimation error for $X(k+1|k-1)$ and the predication $Y(k|k-1)$ can be proved. According to the orthogonal theorem, the estimation $X(k|k-1)$ is orthogonal with its estimation error as shown in Eq.22.

$$E\left\{X_e\left(k\mid k-1\right)\hat{X}^T\left(k\mid k-1\right)\right\}=0 \tag{22}$$

The online dynamic equalization adjustment of high-power LIB packs based on the SOB estimation is conducted by Wang et al. (2016). The fast SOC estimation is studied by Wu et al. (2014) for LIBs. The SOC estimation is conducted by Xia et al. (2015) for LIBs using an adaptive cubature KF algorithm. The comparisons of modeling and SOC estimation for LIBs are studied by Xiao et al. (2016) based on fractional order and integral order methods. Then, the estimation error for $X(k+1|k-1)$ is also orthogonal with the estimation $X(k|k-1)$ because of the equation shown in Eq.23.

$$E\left\{X_e\left(k+1\mid k-1\right)X_e{}^T\left(k\mid k-1\right)\right\}=E\left\{\left[\Phi\left(k+1,k\right)X_e\left(k\mid k-1\right)+\Gamma\left(k+1,k\right)W\left(k\right)\right]\left[H\left(k\right)\hat{X}\left(k\mid k-1\right)\right]^T\right\} \tag{23}$$

As a result, if the new observation value $Y(k)$ equals the estimation value $Y(k|k-1)$, the estimation $X(k+1|k-1)$ should be the optimal linear prediction of $X(k+1)$. The recursive bayesian filtering framework is constructed by Tagade et al. (2016) for LIB cell state estimation. The accurate and versatile simulation of transient voltage profile of LIB employing internal ECM is studied by Tanaka et al. (2015). The SOC estimation of a LIB cell is conducted by Tanim et al. (2015) based on a temperature dependent and electrolyte enhanced single particle model. The similarity recognition of online data curves based on dynamic spatial time warping is studied by Tao et al. (2015) for the estimation of LIB capacity. Actually, the parameter Z(k) cannot just equal to the estimation value $Y(k|k-1)$, the usual value of which can be described as shown in Eq.24.

$$Y\left(k\right)=H\left(k\right)X\left(k\right)+V\left(k\right)=H\left(k\right)\left[\hat{X}\left(k\mid k-1\right)+X_e\left(k\mid k-1\right)\right]+V\left(k\right) \tag{24}$$

An adaptive gain nonlinear observer is constructed by Tian et al. (2014) for the SOC estimation of LIBs in EVs. The SOC estimation is conducted by Xing et al. (2014) for LIBs using the OCV at various ambient temperatures. The correlation between SOC and Coulombic efficiency is studied by Zheng et al. (2015) on for commercial LIBs. Then, the prediction error for $Y(k)$ can be calculated as shown in Eq.25.

$$Y_e\left(k\mid k-1\right)=Z\left(k\right)-\hat{X}\left(k\mid k-1\right)=H\left(k\right)X_e\left(k\mid k-1\right)+V\left(k\right) \tag{25}$$

The reasons of producing this estimation error are that: (1) the prediction for $X(k|k-1)$ which is done for the state vector $X(k)$ at k time point has estimation error; (2) the white noise interference $V(k)$ is attached. This estimation error should be used to correct the prediction of the state vector $X(k+1)$ at k time point appropriately. As a result, the linear estimation and weighted method is usually used for the calibration process. In addition, it is sensitive to initial error convergence state estimation error and inaccurate estimation matrix may cause the filter divergence and affect its stability. In order to overcome this disadvantage in the SOC estimation process, the improved EKF-based compromising is a necessary part of constructing the ECM estimation model into practice. By adding a correcting parameter that is proportional to the estimation error of $Y(k|k-1)$, the follow equation can be obtained as shown in Eq.26.

$$\hat{X}\left(k+1\mid k\right)=\Phi\left(k+1,k\right)\hat{X}\left(k\mid k-1\right)+K\left(k\right)Y_e\left(k\mid k-1\right) \tag{26}$$

The robust and adaptive estimation of SOC is conducted by Zhang et al. (2015) for LIBs. An online SOC estimation method proposed by Xu et al. (2014) with reduced prior battery testing information. A comparative study of three model-based algorithms for estimating the SOC value of LIBs under a new combined dynamic loading profile is conducted by Yang et al. (2016). By the combined application of above two equations, the equation can be transformed as shown in Eq.27.

$$\hat{X}\left(k+1|k\right)=\Phi\left(k+1,k\right)\hat{X}\left(k|k-1\right)+K\left(k\right)\left[Z\left(k\right)-H\left(k\right)\hat{X}\left(k|k-1\right)\right] \tag{27}$$

A multi time-scale SOC and SOH estimation framework is constructed by Yin et al. (2015) using nonlinear predictive filter for LIB pack with passive balance control. The SOC estimation is conducted by Yu et al. (2015) for LIBs using a KF based on local linearization. The stability analysis for LIB model parameters and SOC estimation by measurement uncertainty consideration is conducted by Yuan et al. (2015). Wherein, the $K(k)$ is a undetermined matrix which is named as optimal gain matrix or weighted matrix that is shown in Eq.28.

$$\hat{X}\left(k+1|k\right)=\Phi\left(k+1,k\right)\hat{X}\left(k|k-1\right)+K\left(k\right)H\left(k\right)X_{e}\left(k|k-1\right)+K\left(k\right)V\left(k\right) \tag{28}$$

A data-driven based adaptive SOC estimator of LIB is constructed by Xiong et al. (2014) used in EVs. The SOC estimation is conducted by Xu et al. (2014) for the LIBs based on a proportional-integral observer. An integrated approach is proposed by Zhang et al. (2015) for real-time model-based SOC estimation of LIBs. As the system state function at k+1 time point is set as shown in the second part of Eq.21, the estimation error of $X(k+1)$ can be obtained as shown in Eq.29.

$$X_{e}\left(k+1|k\right)=X\left(k+1\right)-\hat{X}\left(k+1|k\right)=\left[\Phi\left(k+1,k\right)-K\left(k\right)H\left(k\right)\right]X_{e}\left(k|k-1\right)+\Gamma\left(k+1,k\right)W\left(k\right)-K\left(k\right)V\left(k\right) \tag{29}$$

For the right part of the equation, the parameters of $W(k)$, $V(k)$ and the estimation error of $X(k|k\text{-}1)$ are all orthogonal to observation vector $Y(0)$, $Y(1)$, …, $Y(k\text{-}1)$, so the estimation error for $X(k+1|k)$ is also orthogonal to the observation vector. If the estimation error of $X(k+1|k)$ is also orthogonal to $Y(k)$, the estimation of $X(k+1|k)$ will be the optimal linear prediction of $X(k+1)$. As a result, the orthogonal condition between the estimation error of $X(k+1)$ and $Z(k)$ as shown in Eq.30, which can be used to determine the undetermined optimal gain matrix $K(k)$.

$$E\left\{X_{e}\left(k+1|k\right)Y^{T}\left(k\right)\right\}=0 \tag{30}$$

The EKF method is used by Xiong et al. (2014) for the SOC estimation of vanadium redox flow battery using thermal-dependent electrical model. A data-driven based adaptive SOC estimator of LIB used in EVs. By introducing the estimation error of $X(k+1|k)$ as shown in Eq.28 and the observation vector function as shown in Eq.25, the follow equation can be obtained.

$$\begin{aligned}&E[\left\{\left[\Phi\left(k+1,k\right)-K\left(k\right)H\left(k\right)\right]\hat{X}\left(k|k-1\right)+\Gamma\left(k+1,k\right)W\left(k\right)-K\left(k\right)V\left(k\right)\right\}\\&\left\{H\left(k\right)\left[\hat{X}\left(k|k-1\right)+\hat{X}\left(k|k-1\right)\right]+V\left(k\right)\right\}^{T}]=0\end{aligned} \tag{31}$$

Considering that the estimation $X(k|k\text{-}1)$ and its estimation error, together with the parameters of $W(k)$ and $V(k)$ are all orthogonal with each other, the above equation can be simplified as shown below.

$$E\left\{\left[\Phi\left(k+1,k\right)-K\left(k\right)H\left(k\right)\right]X_{e}\left(k|k-1\right)X_{e}^{T}\left(k|k-1\right)H^{T}\left(k\right)-K\left(k\right)V\left(k\right)V^{T}\left(k\right)\right\}=0 \tag{32}$$

The vector $P(k|k\text{-}1)$ can be used to describe the estimation error variance matrix as shown in Eq.33.

$$\begin{cases}P\left(k|k-1\right)=E\left\{X_{e}\left(k|k-1\right)X_{e}^{T}\left(k|k-1\right)\right\}\\E\left\{V\left(k\right)V^{T}\left(k\right)\right\}=R_{k}\end{cases} \tag{33}$$

A SOC estimation method can be proposed for the LIB pack based on in-pack cells uniformity analysis and the follow equation can be obtained.

$$\left[\Phi\left(k+1,k\right)-K\left(k\right)H\left(k\right)\right]P\left(k|k-1\right)H^{T}\left(k\right)-K\left(k\right)R_{k}=0 \tag{34}$$

A data-driven bias-correction-method-based LIB modeling approach can be obtained by the above calculating process and the optimal gain matrix can be calculated as shown in Eq.35.

$$K\left(k\right)=\Phi\left(k+1,k\right)P\left(k|k-1\right)H^{T}\left(k\right)\left[H\left(k\right)P\left(k|k-1\right)H^{T}\left(k\right)+R\left(k\right)\right]^{-1} \tag{35}$$

Then, it is necessary to determine the recursion formula of the estimation variance matrix $P(k+1|k)$. According to the definition, the description of the estimation variance matrix is shown in Eq.36.

$$P(k+1|k)=E\left\{X_e(k+1|k)X_e^T(k+1|k)\right\} \tag{36}$$

However, if the system is nonlinear, linear processing in each step, which is used for linear approximation of nonlinear systems varying systems. As a result, it is necessary to use this linearization process for the non-linear system of the power LIB. The state and measurement equations in the modeling of the nonlinear LIB system and calculation procedures are shown in Eq.37.

$$\begin{cases} X(k+1)=f\left\{X(k),U(k)\right\}+w(k) \\ Y(k+1)=g\left\{X(k),U(k)\right\}+v(k) \end{cases} \tag{37}$$

Wherein, the first part of Eq.37 represents all the system dynamics expressed in state equations and the second part of it indicates the system measurement equation with a static relationship. The function $f\{X(k),U(k)\}$ is a nonlinear transition function and the function $g\{X(k),U(k)\}$ is a nonlinear measurement function. The vectors $w(k)$ and $v(k)$ denote process and measurement noise which are uncorrelated zero-mean white Gaussian stochastic processes with covariance matrixes Q and R respectively. At each time step, the linearization is done for the matrices of $f\{X(k),U(k)\}$ and $g\{X(k),U(k)\}$ which are close to the operation point by the first order in Taylor-series and the rest series are truncated.

3. Experimental results and discussion

In order to verify the validity of the proposed method, the BMTS equipment is designed and used for the aerial LIB packs, aiming to perform the aerial environmental conditions for subsequent experiments and shown in Fig.5.

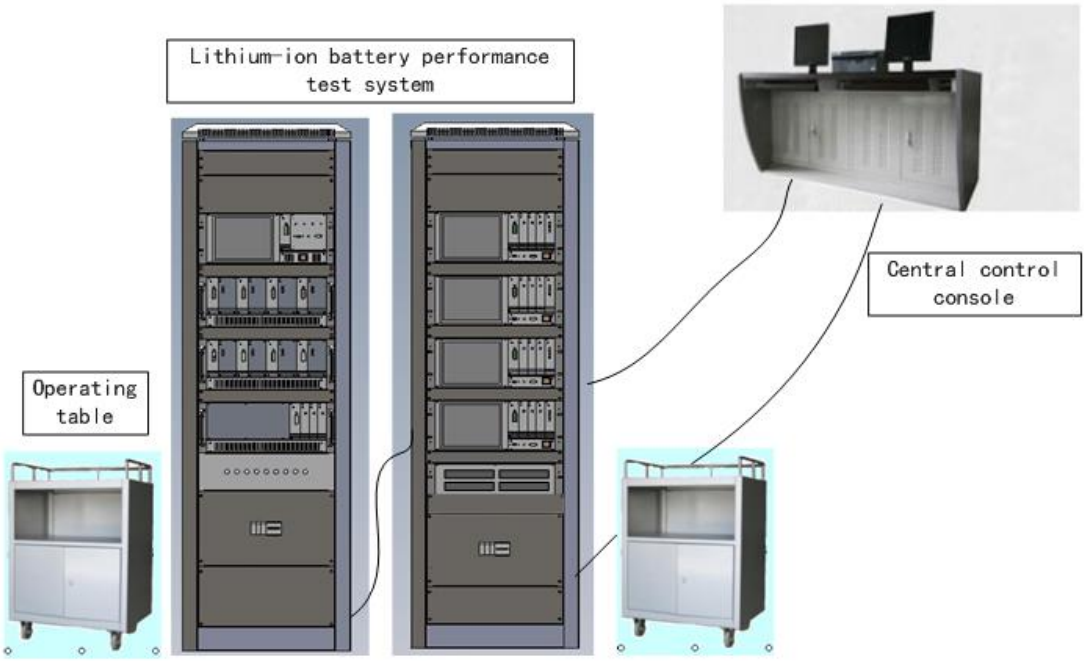

Fig. 5. The BMTS designed for the LIB packs

As shown in above figure, the DC power supply is used to simulate the antenna output power and DC electronic load simulation loading system. The data acquisition subsystem is designed to record the voltage, current and temperature characteristics, which is used for computing the on-chip reference system. The high-precision current sensors are used for the on-chip reference chip system, the current accuracy of which is between 0.10% and 0.15%. The C# type program is used to control the hardware devices. The hot chamber is used to maintain the temperature of the LIB to be about 23 ℃ to keep the temperature stable for the aerial application. The comparative data processing and real-time test systems use the dsPIC6014A as the acquired microcontroller. In addition, the internal resistance tester is designed for the further reference. The SOC estimation model is designed and used as shown in

Fig.6, in which the factors of current density, temperature, Coulombic efficiency and other parameters are considered in the estimation process.

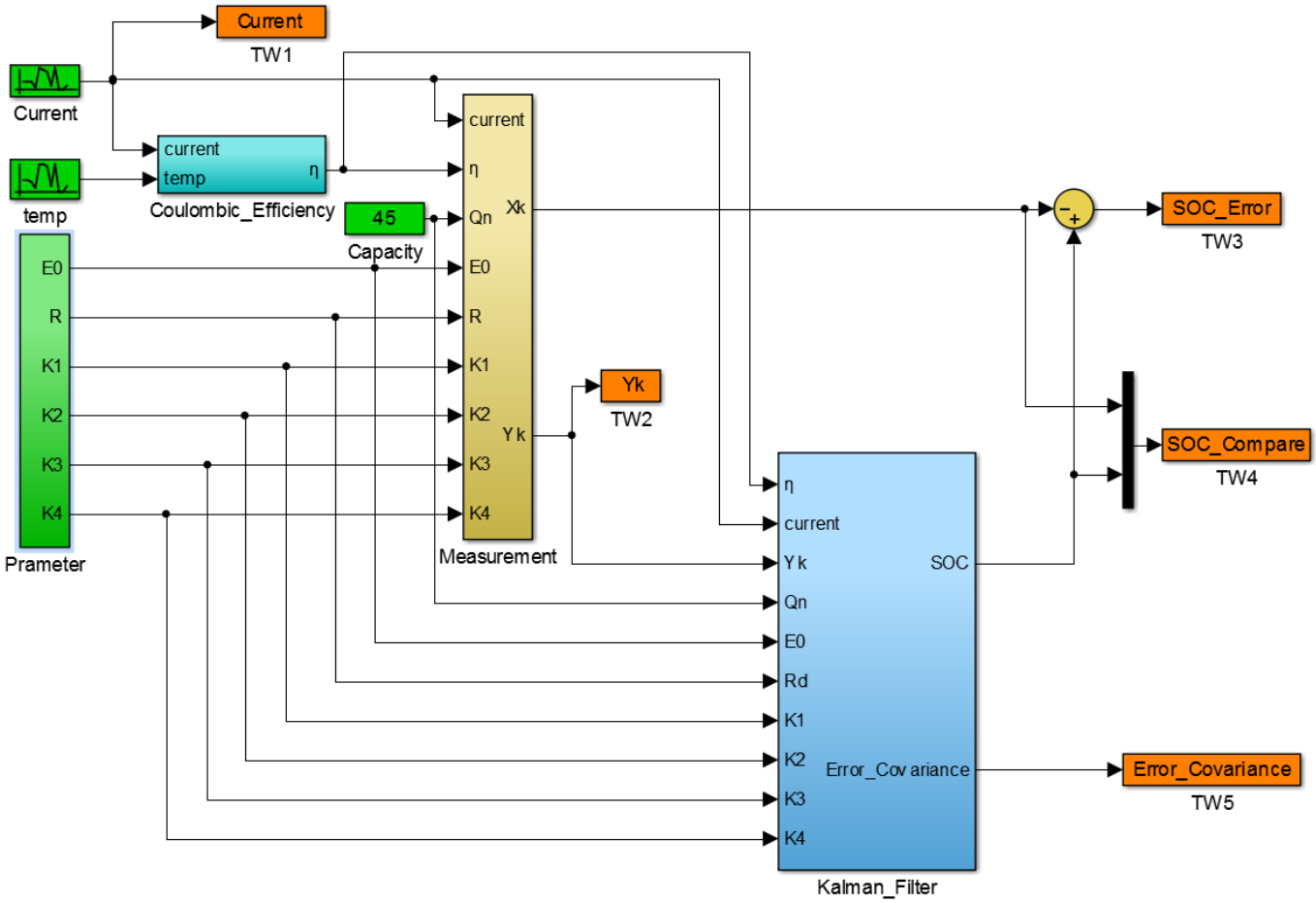

Fig. 6. The SOC estimation model with multi-factors

In the LIB pack, the storage of energy and energy transfer capability are important, so the system-level chip is highly dependent on the performance of individual cells and chips, in which electrical topology and balance control are very important. In this work, the state estimation problems of the LIB pack using cells in series consisting of configuration are particularly considered. The ability to define the concept of extending the package into a single cell level definitions, packaging capacity is the total ampere hours from the rechargeable battery in the LIB pack until the pack is fully discharged and the LIB packs with 7-ICP series are used as the experimental samples.

3.1. Discharging voltage characteristics

The following diagram depicts the same type of LIB cell terminal voltage different fading characteristics of CC charge and discharge rates. The voltage drop rate is different from the cross-flow of the various discharge rates (i.e., different discharge currents) of the maintenance procedure. After changing the LIBs by CC-CV method, the LIB needs to be placed on hold to obtain the charging maintenance voltage to enhance the terminal voltage to be stable between the electrodes. And the discharge voltage characteristics under different discharge rates are measured and analyzed. When doing the discharge test, the discharging terminal voltage reaches the discharging cutoff voltage, which is set to be 3.0V at different discharge currents. Experiments are performed at different ambient temperatures and different discharging rates, and the discharging voltage curves corresponding to the final properties are obtained. The different discharge voltage - time curves can be obtained by modeling the experimental environment in different discharge rates. The discharge voltage characteristics of different discharge rates are shown in Fig. 7.

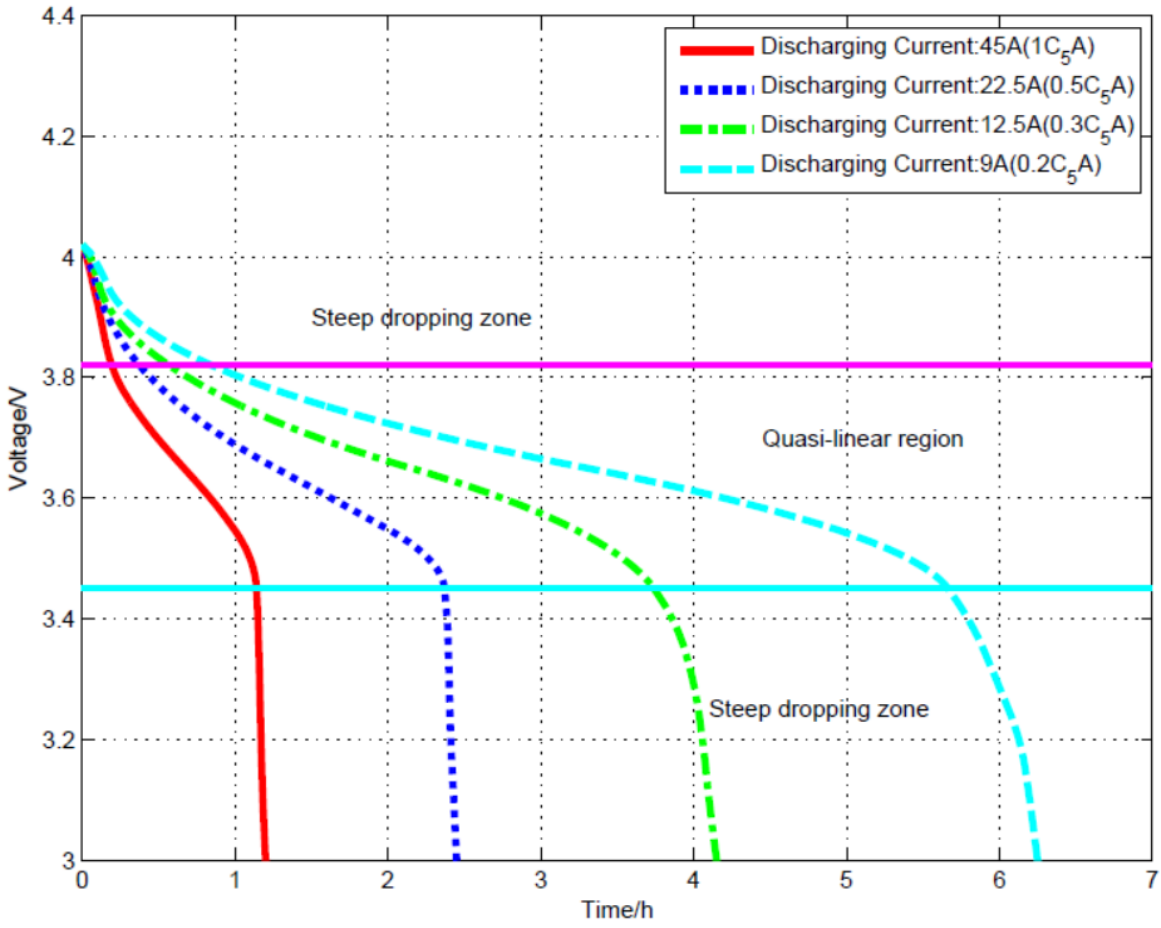

Fig. 7. Discharging voltage characteristics

The above graph can be divided into three regions, namely 1 (steep drop zone), 2 (linear region), and 3 (steep drop zone), which are separated from the three solid lines. As can be seen from the above figure, the voltage dropped drastically over time firstly. In the second district, the voltage decreases slowly with time. At the third zone, the sudden voltage drop happens to be the minimum threshold value. In the energy supply process, most of the working time is in the second region and only a small part of working hours in the first and three time areas. Fortunately, this phenomenon is what we want to see. In the presence of a radical LIB hysteresis, the radicals are several possible reasons for the thermodynamic equilibrium potential, corresponding to a positive electrode and lithium cobalt oxide as the active material which is known from the exhibit hysteresis. The particles and OCV potentials are corresponding to the chemical potential of SOC which may be different depending on the composition of the particles. In addition, the lithium graphite anode is a complex process, which is dependent on the path and provide help to further lag.

For free parameters extracted under various experimental DCM mounts different SOC injection interval detection and the corresponding voltage responses. In order to obtain the desired voltage response, freedom is by using CC-CV charging method, which is half an hour $0.2C_5A$ periodically removed half hour break. At each time interval of rest, different charge and discharge current pulses with duration of 10 seconds is injected into the library. Suppose the open circuit voltage U_{OC} parameters in a short time constant, the corresponding voltage response with respect to each recording pulse current. Repeat at intervals of 5% every time a system until the free library is fully released. On different chip voltage response current pulse is injected, and then used in the identification and recognition of the transfer function. With the corresponding current pulse voltage response, the coefficient parameters of A_2, A_1, A_0 and B_0, B_1 of the transfer function $G(s)$ can be calculated with reasonable values. Then, the parameters of R_Ω, R_P and C_P can be obtained by solving these coefficients, which are shown in Eq.38.

$$R_{\Omega} = 26m\Omega; R_P = 10m\Omega; C_P = 300F \quad (38)$$

Different transfer functions and parameter sets are determined in each of the detected voltage at the system level. Due to parameter changes, it is respected to consider the negligible organic carbon and the average determined parameters. The HPPC load curve is used to verify the determined parameters, in which the experimental value of the voltage and the estimation errors are compared and analyzed. The results showed that the parameters of the state-space model can determine an accurate estimation of the terminal voltage for the aerial LIB pack. The average estimation error is less than 8mV and the maximum error is 43mV in the charge and discharge pulse. The important indicators of working status are used in the two working areas for the length of time scope of the LIB pack. At different discharge rates, the LIB working time is divided in two different zones. In the process of evaluating the SOC value of the LIB pack, it should be a different type of processing power or energy application environment and can be carried out a detailed analysis and evaluation that should be done.

3.2. Discharging capacity characteristics

Experiments at different temperatures (-20℃, -10℃, 0℃,10℃, 20℃, 60℃) and different CC discharge current for the LIB pack samples. All-electric SOC values are considered from the last record to the discharge terminal voltage together with the battery capacity obtained by experiments and thus the total energy can be released. As can be seen from different experiments, the battery discharge rate has a constant affect on the final released energy. With the impact of this effect, the performance is evident at a relatively low temperature, such as 0 degrees Celsius. As can be seen from the experimental results, that the high-capacity LIB discharge rate almost has no effect on the size of capacity, when the temperature is greater than 0 °C. However, the LIB capacity increased significantly when reducing the temperature and the discharge rate, in which the temperature is lower than 0 ° C. That is to say, the LIB will has less emission rate and greater release capacity when the temperature is low.

A possible method of estimating the OCV value for the LIB is to do the DCM process with a small current, and use the average voltage value as the OCV value, which is obtained from the measurement voltages detected during the charging and discharging process. As a result, the low current can be applied to minimize the diffusion-limited. However, even at lower current DCM, the contribution of the LIB battery experiences dynamics is almost fully charged due to electrical discharge or high voltage and a measured voltage OCV cannot be assumed to be more free. The discharge capacity law of the LIB released from a full power state is shown in Fig. 8.

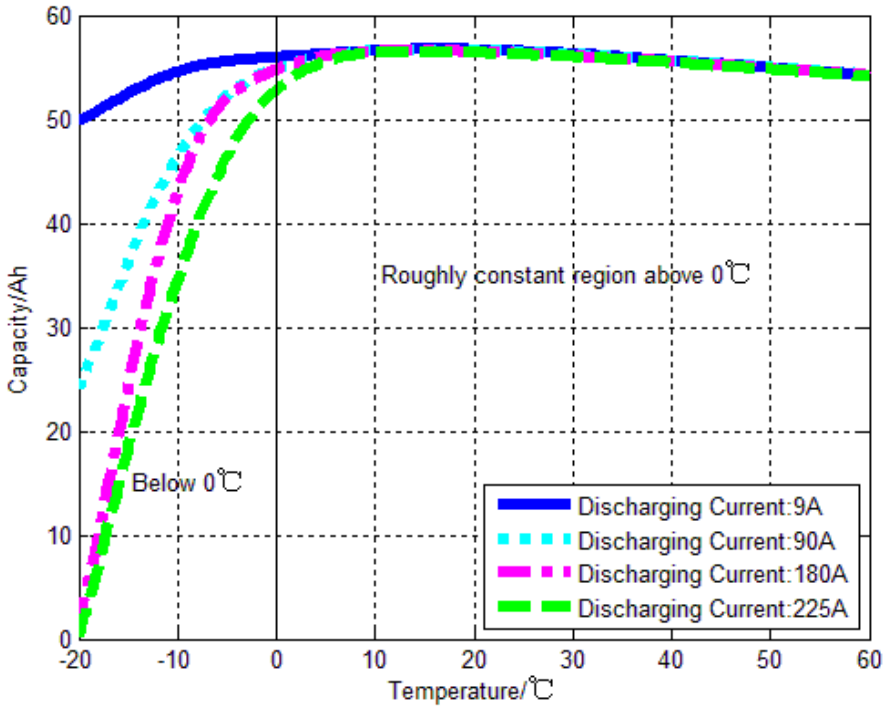

Fig. 8. Battery discharging capacity from full power status

The impact effects of the discharge capacity are analyzed under different discharge rates (1C, 10C, 20C, and 25C). Basically, the LIBS higher the temperature, the larger discharge capacity. For example, the impact on the 1C rate discharge capacity of ambient temperature, as shown below, mainly for 9A discharge current curve. As we have seen, the digital whole area is divided into 0 partial longitudinal axis, in degrees Celsius. The model-based dynamic power assessment is conducted by Hu et al. (2014) for the LIBs considering different operating conditions. When the temperature is higher than 0 °C, the capacity is with little change in the variation on discharging rates and environmental temperatures. The SOC estimation for the LIB is conducted by Li et al. (2015) based on strong tracking sigma point KF algorithm. When the temperature is below 0 °C, when the temperature is below 0 °C, with the discharge rate and temperature changes, changes in the larger capacity. As described above, the discharge capacity of the battery from full power is released to the discharge terminal voltage. Herein, the acquisition process is described as shown in Fig. 9.

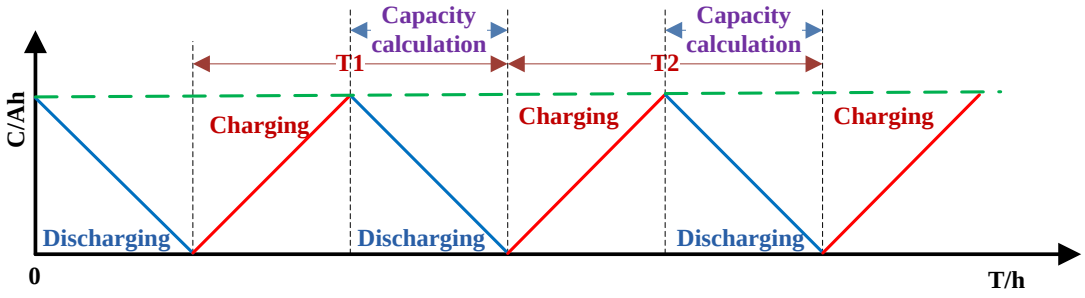

Fig. 9. Remaining capacity cycle calculation process

The parameters of T_1 and T_2 in the above figure indicate the charging and discharging cycle time period. As we can see, the capacity will be calculated from the highest point of the lowest point in the figure. The SOC estimation is conducted by He et al. (2014) for the LIBs using NN modeling and UKF-based error cancellation. The online

estimation of LIB capacity using sparse Bayesian learning is conducted by Hu et al. (2015). The capacity cycling maintenance test is also done by Yin H et al. (2015) as shown in Fig.13 and has similar experimental process.

3.3. Capacity degradation of the LIB

With the aging influence, the capacity of LIB will decrease, but there is no clear conclusion mechanism that exists in the attenuation process. The degradation data is analyzed for the SOC estimation process by means of correct the realistic capabilities of the LIB. The following diagram is the cycling life test results by discharging it at $1C_5A$ rate at room temperature. By analyzing the actual capacity and the corresponding cycle number of the LIB, as can be seen from the following figure, the LIB capacity is changed in a certain number of DCM cycles. When the LIB cycling number is changed, the capacity value of the LIB will change along with it. By doing the DCM with 1C discharge rate under the normal temperature conditions, the relationship between the capacity of LIB and the corresponding cycle number is described as shown in Fig. 10.

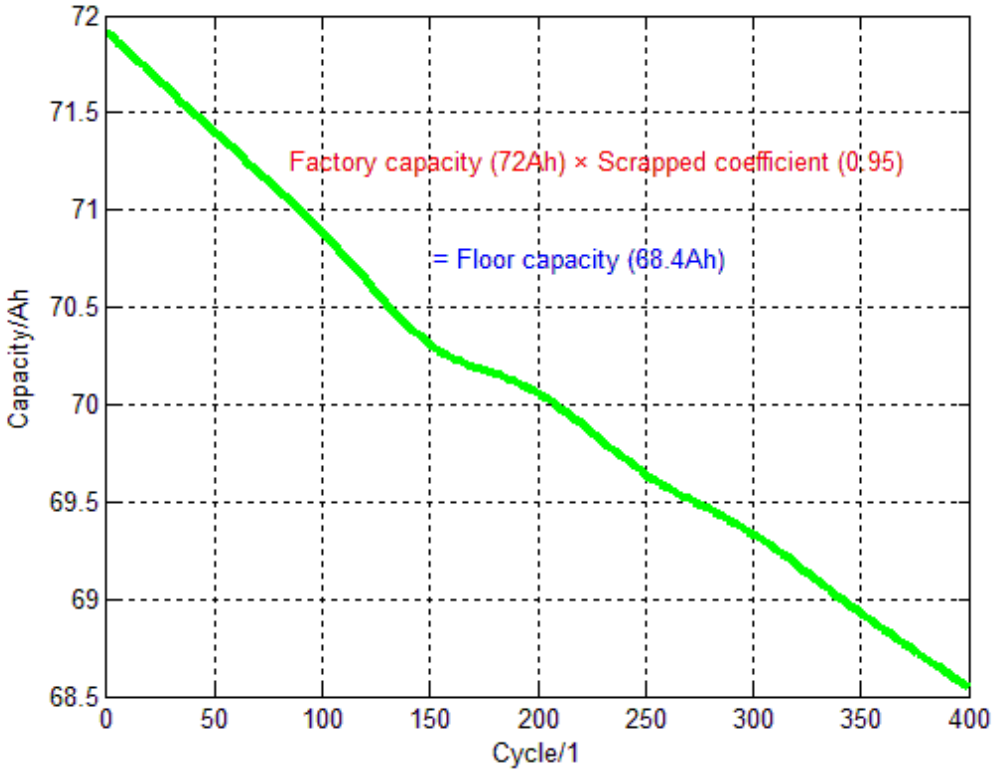

Fig. 10.Relationship between capacity and cycle numbers

The SOC estimation accuracy can be influenced by the impact of the ECM parameters, which are depending on the cellular changes in the internal structure of the LIB. As the LIB usage increases, the processing parameters such as R_Ω will change along with it. The SOC algorithm and its associated model are related to the existing data and altitude experimental data of the aerial LIB with ICP series. By the comparison of experimental data and the rated battery data, the adaptability of the algorithm is analyzed. The SOC estimation is conducted by Hua et al. (2015) for two types of LIBs using the nonlinear predictive filter for EVs. These parameters are considered as a state of the LIB power supply system, it is estimated by the nonlinear observer discrete values, and the relationship between these parameters are obtained from the experimental data of the battery capacity.

3.4. The SOC estimation characteristics

The SOC estimation method, considering the LIB characteristics, is verified by doing the DCM process and the experimental results are compared with other SOC estimation methods. Estimation performance estimation method utilizing the proposed on-chip system. True system on a chip set to 100% and an initial estimation value of 90%.

Experimental results show that the estimated SOC converges to real values in over 50 years of age, the initial estimate of SOC is set to an initial value is not accurate. To further verify the convergence performance of the proposed method of estimation error during the entire discharge system on a chip are summarized. Experimental results show that the proposed method is able to converge to the maximum estimation error over the entire operating range of 4.23%. The results showed that the initial estimation error does not affect the convergence of SOC estimated using the ECM-EKF methods. As the structure of LIB materials has changed, it should also experience behavioral changes in mathematics. The SOC performance factor of LIB is described by actual SOC chart. Therefore, it is necessary to provide charge-discharge characteristics of the LIB. The performance test data is analyzed and the parameter identification model is designed to obtain the charging and discharging parameters for the accurate extraction in the useful parameter characterization process of LIB. Temperature, voltage, current, aging and other factors are used to estimate the SOC characteristics accurately in the application of associated BMS system of the aerial LIB pack. The SOC estimation results are compared with the experimental results when doing the discharging process as shown in Fig. 11, which has similar regulation with the experimental results obtained by Zhang CH et al. (2014).

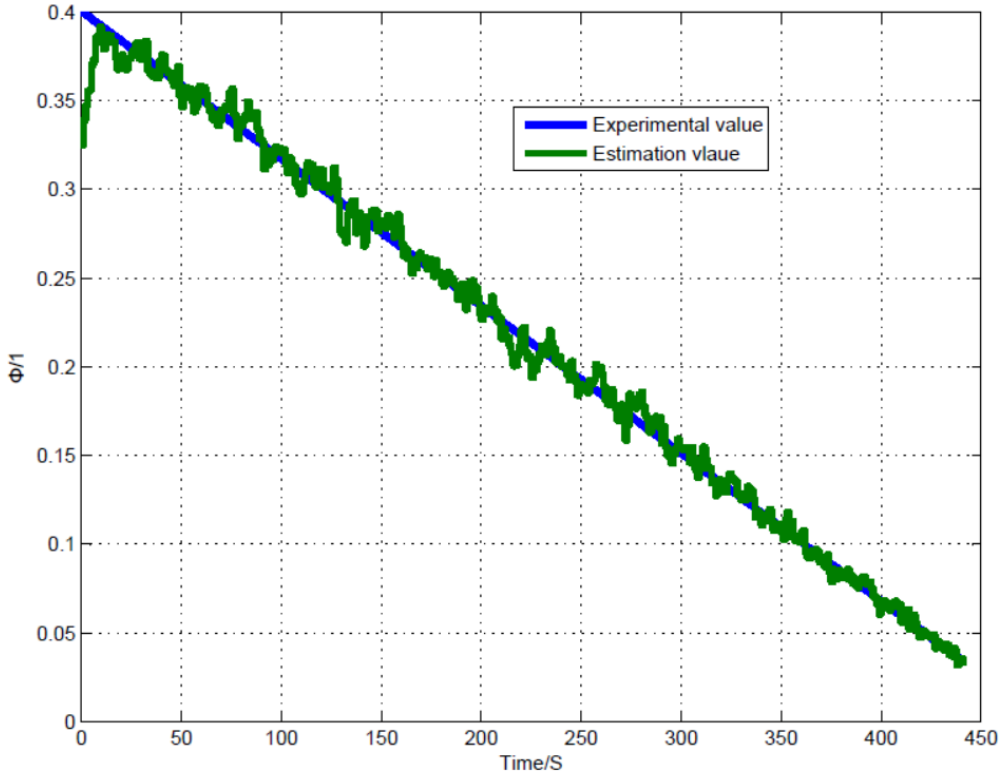

Fig. 11. SOC estimating normalization characteristics

As can be seen from the experimental results, it can be observed on the basis of Coulomb counting algorithm from the on-chip system referenced to the accumulation of errors. In order to evaluate the different performance of the SOC estimation methods, the absolute average, maximum error and RMSE is calculated according to the formula as shown in Eq.39.

$$\begin{cases} Mean = \dfrac{1}{n}\sum_{k=1}^{n}\left|SOC(k) - SOC(k)\right|, MaxErr = Max\left|SOC(k) - SOC(k)\right| \\ RMSE = \sqrt{\dfrac{1}{n}\sum_{k=1}^{n}\left[SOC(k) - SOC(k)\right]^2} \end{cases} \tag{39}$$

The percentage error of the estimated percentage increase from its Coulomb counting error can be observed linear, because the error accumulation. Experimental results show that, the proposed SOC estimation method has a lower

average absolute, absolute maximum and RMSE than all other methods. In addition, it is more effective than other model-based estimation methods.

3.5. SOC estimation based on the improved EKF algorithm

In this study, the correlation is used to model the experimental data and the parameters of the battery and the least square fitting method is used between the OCV and SOC values. The relationship between the OCV and SOC is obtained, which is also characterized by using the least square fitting method with 7-order equation. The detection data and the fitting curve are shown in Fig. 12, according to which the resistance and electrical capacity values used in the ECM can be obtained.

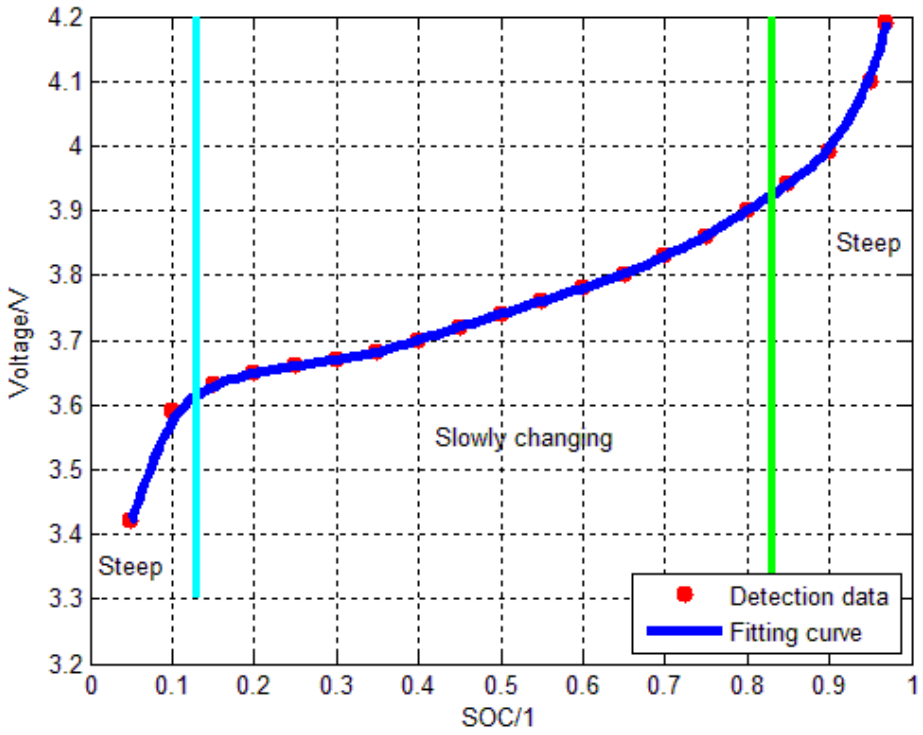

Fig. 12.Least-square fitting for the voltage and SOC

The result of fitting various OCV relaxation models to the OCV relaxation curve measured for LIBs is also obtained by Waag W et al. After obtaining the estimated parameters using the EKF method combined with the battery model estimation, the battery SOC estimation model combined with the EKF is tested. The real-time estimation is conducted by He et al. (2016) for the battery SOC with UKF and RTOS mu COS-II platform. Experimental results show that the value of a high concentration obtained SOC credibility integrated SOC estimation method based reasoning. The comprehensive SOC evaluation strategy method is used to determine the accuracy of greater than 90%, indicating that the method can effectively estimation. This comprehensive system based on SOC estimation method can work well.

4. Conclusion

In this study, a new and powerful SOC estimation method is proposed by using the construction and application of the ECM-EKF estimation model. The proposed estimation method is based on linear matrix advantage of utilization. In addition, the square root characteristics of the proposed method can improve the state covariance value property. The pulsed power characteristics of the test results and OCV curve can verify the system performance. The estimation accuracy can be regarded as superior to existing publications. Experimental results show that the proposed method can achieve the comprehensive evaluation based on the credibility reasoning of LIBs. By using the proposed SOC estimation method, a verification system is established with the implementation

of a new estimation model. The integrated SOC estimation model can work well for LIBs, effectively ensuring the reliability of the battery-powered applications. It has beneficial effects on the promotion and application of high power LIB packs.

Acknowledgments

The work was supported by the Sichuan Science and Technology Support Program (No. 2014GZ0078) and the Mianyang Science and Technology Project (No. 15G-03-3). And the early work was supported by the Photoelectric detection technology and application projects (No. 12zd1105 and No. 12TD006) and the Special environment integrated testing - Laboratory Robotics Project (No. 13zxtk0502). We would like to thank the sponsors.

References

[1] Aung H, Low KS, Goh ST. State-of-charge estimation of lithium-ion battery using square root spherical unscented Kalman filter (Sqrt-UKFST) in nanosatellite. IEEE Transactions on Power Electronics 2015; 30(9): 4774-4783.

[2] Aung H, Low KS. Temperature dependent state-of-charge estimation of lithium ion battery using dual spherical unscented Kalman filter. IET Power Electronics 2015; 8(10): 2026-2033.

[3] Barai A, Widanage WD, Marco J. A study of the open circuit voltage characterization technique and hysteresis assessment of lithium-ion cells. Journal of Power Sources 2015; 295: 99-107.

[4] Bartlett A, Marcicki J, Onori S. Electrochemical model-based state of charge and capacity estimation for a composite electrode lithium-ion battery. IEEE Transactions on Control Systems Technology 2016; 24(2): 384-399.

[5] Bazinski SJ, Wang X. Experimental study on the influence of temperature and state-of-charge on the thermophysical properties of an LFP pouch cell. Journal of Power Sources 2015; 293: 283-291.

[6] Chen XP, Shen WX, Dai MX. Robust adaptive sliding-mode observer using RBF neural network for lithium-ion battery state of charge estimation in electric vehicles. IEEE Transactions on Vehicular Technology 2016; 65(4): 1936-1947.

[7] Corno M, Bhatt N. Electrochemical model-based state of charge estimation for Li-ion cells. IEEE Transactions on Control Systems Technology 2015; 23(1): 117-127.

[8] Dang XJ, Yan L, Xu K. Open-circuit voltage-based state of charge estimation of lithium-ion battery using dual neural network fusion battery model. Electrochimica Acta 2016; 188: 356-366.

[9] Dong GZ, Wei JW, Zhang CB. Online state of charge estimation and open circuit voltage hysteresis modeling of LiFePO4 battery using invariant imbedding method. Applied Energy 2016; 162: 163-171.

[10] Gao JP, Zhang YZ, He HW. A real-time joint estimator for model parameters and state of charge of lithium-ion batteries in electric vehicles. Energies 2015; 8(8): 8594-8612.

[11] Gong XZ, Xiong R, Mi CC. A data-driven bias-correction-method-based lithium-ion battery modeling approach for electric vehicle applications. IEEE Transactions on Industry Applications 2016; 52(2): 1759-1765.

[12] He HW, Xiong R, Peng JK. Real-time estimation of battery state-of-charge with unscented Kalman filter and RTOS mu COS-II platform. Applied Energy 2016; 162: 1410-1418.

[13] He W, Williard N, Chen CC. State of charge estimation for Li-ion batteries using neural network modeling and unscented Kalman filter-based error cancellation. International Journal of Electrical Power & Energy Systems 2014; 62: 783-791.

[14] Hu C, Jain G, Schmidt C. Online estimation of lithium-ion battery capacity using sparse Bayesian learning. Journal of Power Sources 2015; 289: 105-113.

[15] Hu XS, Xiong R, Egardt B. Model-based dynamic power assessment of Lithium-ion batteries considering different operating conditions. IEEE Transactions on Industrial Informatics 2014; 10 (3): 1948-1959.

[16] Hua Y, Xu M, Li M. Estimation of state of charge for two types of lithium-ion batteries by nonlinear predictive filter for electric vehicles. Energies 2015; 8(5): 3556-3576.

[17] Kim T, Wang YB, Fang HZ. Model-based condition monitoring for lithium-ion batteries. Journal of Power Sources 2015; 295: 16-27.

[18] Kuo TJ, Lee KY, Huang CK. State of charge modeling of lithium-ion batteries using dual exponential functions. Journal of Power Sources 2016; 315: 331-338.

[19] Lee S, Kim J. Discrete wavelet transform-based denoising technique for advanced state-of-charge estimator of a lithium-ion battery in electric vehicles. Energy 2015; 83: 462-473.

[20] Li D, Ouyang J, Li HQ. State of charge estimation for LiMn2O4 power battery based on strong tracking sigma point Kalman filter. Journal of Power Sources 2015; 279: 439-449.

[21] Lim DJ, Ahn JH, Kim DH. A mixed SOC estimation algorithm with high accuracy in various driving patterns of EVs. Journal of Power Electronics 2016; 16(1): 27-37.

[22] Lim K, Bastawrous HA, Duong VH. Fading Kalman filter-based real-time state of charge estimation in LiFePO4 battery-powered electric vehicles. Applied Energy 2016; 169: 40-48.

[23] Lin C, Mu H, Xiong R. A novel multi-model probability battery state of charge estimation approach for electric vehicles using H-infinity algorithm. Applied Energy 2016; 166: 76-83.

[24] Lin XF, Stefanopoulou AG, Anderson RD. State of charge imbalance estimation for battery strings under reduced voltage sensing. IEEE Transactions on Control Systems Technology 2015; 23(3): 1052-1062.
[25] Lu C, Tao LF, Fan HZ. Li-ion battery capacity estimation: A geometrical approach. Journal of Power Sources 2014; 261: 141-147.
[26] Meng JH, Luo GZ, Gao F. Lithium polymer battery state-of-charge estimation based on adaptive unscented Kalman filter and support vector machine. IEEE Transactions on Power Electronics 2016; 31(3): 2226-2238.
[27] Nejad S, Gladwin DT, Stone DA. A systematic review of lumped-parameter equivalent circuit models for real-time estimation of lithium-ion battery states. Journal of Power Sources 2016; 316: 183-196.
[28] Sepasi S, Ghorbani R, Liaw BY. A novel on-board state-of-charge estimation method for aged Li-ion batteries based on model adaptive extended Kalman filter. Journal of Power Sources 2014; 245: 337-344.
[29] Sepasi S, Ghorbani R, Liaw BY. Improved extended Kalman filter for state of charge estimation of battery pack. Journal of Power Sources 2014; 255: 368-376.
[30] Shao S, Bi J, Yang F. On-line estimation of state-of-charge of Li-ion batteries in electric vehicle using the resampling particle filter. Transportation Research Part D: Transport and Environment 2014; 32: 207-217.
[31] Shi W, Wang JL, Zheng JM. Influence of memory effect on the state-of-charge estimation of large format Li-ion batteries based on LiFePO4 cathode. Journal of Power Sources 2016; 312: 55-59.
[32] Tagade P, Hariharan KS, Gambhire P. Recursive bayesian filtering framework for lithium-ion cell state estimation. Journal of Power Sources 2016; 306: 274-288.
[33] Tanaka T, Ito S, Muramatsu M. Accurate and versatile simulation of transient voltage profile of lithium-ion secondary battery employing internal equivalent electric circuit. Applied Energy 2015; 143: 200-210.
[34] Tanim TR, Rahn CD, Wang CY. State of charge estimation of a lithium ion cell based on a temperature dependent and electrolyte enhanced single particle model. Energy 2015; 80: 731-739.
[35] Tao LF, Lu C, Noktehdan A. Similarity recognition of online data curves based on dynamic spatial time warping for the estimation of lithium-ion battery capacity. Journal of Power Sources 2015; 293: 751-759.
[36] Tian Y, Chen CR, Xia BZ. An adaptive gain nonlinear observer for state of charge estimation of Lithium-ion batteries in electric vehicles. Energies 2014; 7: 5995-6012.
[37] Tian Y, Xia BZ, Sun W. A modified model based state of charge estimation of power lithium-ion batteries using unscented Kalman filter. Journal of Power Sources 2014; 270: 619-626.
[38] Tong SJ, Klein MP, Park JW. On-line optimization of battery open circuit voltage for improved state-of-charge and state-of-health estimation. Journal of Power Sources 2015; 293: 416-428.
[39] Truchot C, Dubarry M, Liaw BY. State-of-charge estimation and uncertainty for lithium-ion battery strings. Applied Energy 2014; 119: 218-227.
[40] Unterrieder C, Zhang C, Lunglmayr M. Battery state-of-charge estimation using approximate least squares. Journal of Power Sources 2015; 278: 274-286.
[41] Wang LM, Cheng Y, Zou J. Battery available power prediction of hybrid electric vehicle based on improved Dynamic Matrix Control algorithms. Journal of Power Sources 2014; 261: 337-347.
[42] Wang SL, Shang LP, Li ZF. Lithium-ion battery security guaranteeing method study based on the state of charge estimation. International Journal of Electrochemical Science 2015; 10 (6): 5130-5151.
[43] Wang SL, Shang LP, Li ZF. Online dynamic equalization adjustment of high-power lithium-ion battery packs based on the state of balance estimation. Applied Energy 2016; 166: 44-58.
[44] Wang WX, Wu FJ, Zhao K. Elimination of the state-of-charge errors for distributed battery energy storage devices in islanded droop-controlled microgrids. Journal of Power Electronics 2015; 15 (4): 1105-1118.
[45] Wang YG, Wang ZF, Guo KY. The analysis of modeling of dual Kalman filter in Lithium battery SOC estimates. Applied Mechanics and Materials 2014; 513(1): 4294-4297.
[46] Wang YJ, Zhang CB, Chen ZH. An adaptive remaining energy prediction approach for lithium-ion batteries in electric vehicles. Journal of Power Sources 2016; 305: 80-88.
[47] Wijewardana S, Vepa R, Shaheed MH. Dynamic battery cell model and state of charge estimation. Journal of Power Sources 2016; 308: 109-120.
[48] Wu HJ, Yuan SF, Zhang X. Model parameter estimation approach based on incremental analysis for lithium-ion batteries without using open circuit voltage. Journal of Power Sources 2015; 287: 108-118.
[49] Wu LS, Chen HC, Chou SR. Fast estimation of state of charge for Lithium-ion batteries. Energies 2014; 7 (5): 3438-3452.
[50] Xia BZ, Wang HQ, Tian Y. State of charge estimation of Lithium-ion batteries using an adaptive cubature Kalman filter. Energies 2015; 8(6): 5916-5936.
[51] Xiao RX, Shen JW, Li XY. Comparisons of modeling and state of charge estimation for lithium-ion battery based on fractional order and integral order methods. Energies 2016; 9(3): 1-15.
[52] Xia BZ, Chen CR, Tian Y. A novel method for state of charge estimation of lithium-ion batteries using a nonlinear observer. Journal of Power Sources 2014; 270: 359-366.
[53] Xie JL, Ma JC, Sun YD. Estimating the state-of-charge of lithium-ion batteries using an H-infinity observer with consideration of the hysteresis characteristic. Journal of Power Electronics 2016; 16(2): 643-653.

[54] Xing YJ, He W, Pecht M. State of charge estimation of lithium-ion batteries using the open-ciuciut voltage at various ambient temperatures. Applied Energy 2014; 113: 106-115.
[55] Xiong BY, Zhao JY, Wei ZB. Extended Kalman filter method for state of charge estimation of vanadium redox flow battery using thermal-dependent electrical model. Journal of Power Sources 2014; 262: 50-61.
[56] Xiong R, Sun FC, Gong XZ. A data-driven based adaptive state of charge estimator of lithium-ion polymer battery used in electric vehicles. Applied Energy 2014; 113: 1421-1433.
[57] Xu J, Mi CC, Cao BG. The state of charge estimation of lithium-ion batteries based on a proportional-integral observer. IEEE Transactions on Vehicular Technology 2014; 63(4): 1614-1621.
[58] Xu J, Cao BG, Chen Z. An online state of charge estimation method with reduced prior battery testing information. International Journal of Electrical Power & Energy Systems 2014; 63: 178-184.
[59] Yu ZH, Huai RT, Xiao LJ. State-of-charge estimation for Lithium-ion batteries using a Kalman filter based on local linearization. Energies 2015; 8(8): 7854-7873.
[60] Yuan SF, Wu HJ, Ma XR. Stability analysis for li-ion battery model parameters and state of charge estimation by measurement uncertainty consideration. Energies 2015; 8(8): 7729-7751.
[61] Zhang C, Li K, Pei L. An integrated approach for real-time model-based state-of-charge estimation of lithium-ion batteries. Journal of Power Sources 2015; 283: 24-36.
[62] Zhong L, Zhang CB, He Y. A method for the estimation of the battery pack state of charge based on in-pack cells uniformity analysis. Applied Energy 2014; 113: 558-564.